

Sinter-crystallization of a glass obtained from basaltic tuffs

Alexander Karamanov^{a,*}, Sibel Ergul^b, Mustafa Akyildiz^b, Mario Pelino^c

^a *Institute of Physical Chemistry, Bulgarian Academy of Sciences, G. Bonchev Street, Block 11, 1113 Sofia, Bulgaria*

^b *Department of Engineering, University of Cukurova, 01330 Balcali, Adana, Turkey*

^c *Department of Chemistry, Chemical Engineering and Materials, University of L'Aquila, 67040 Monteluco di Roio, L'Aquila, Italy*

Available online 29 October 2007

Abstract

Glass-ceramic materials, obtained by sinter-crystallization of melted alkaline-olivine basaltic tuffs, were investigated. The kinetics of bulk crystallization was evaluated by differential thermal analysis (DTA) at different heating rates. The phase formation and the sintering behavior of glass powders ($<75\ \mu\text{m}$) were studied in air and in nitrogen atmospheres by DTA and dilatometry, respectively. The crystalline phases formed were identified by X-ray diffraction. The DTA traces showed an unusual phase formation behavior with a higher crystallization trend for the bulk samples. The crystallization activation energy was evaluated as $590 \pm 20\ \text{kJ/mol}$ in the range 1080–1110 K. A value of about 3 of the Avrami constant, corresponding to three-dimensional growth on a fixed number of nuclei, was evaluated by Ozawa and Augis–Bennet methods. The densification at low-temperatures is reduced by the intensive crystallization process in both air and nitrogen atmospheres. The sintering starts again at 1150–1250 K. In air atmospheres, due to the FeO oxidation, the sintering temperature increases and the percentage of formed crystal phase decreases by 15–20%.
© 2007 Elsevier B.V. All rights reserved.

Keywords: Crystallization; Glass ceramics; Geology; Alkali silicates; Sintering

1. Introduction

Due to the elevated melting temperatures, the specific thermal treatment and the high cost of pure raw materials, glass-ceramics attain outstanding properties with high production costs. In some cases, however, it is possible to produce glass-ceramics at low melting temperatures, by using cheap raw materials and short production cycles. Typical examples are the iron-rich silicate compositions.

The first iron-rich glassy material was developed before the First World War in the France ‘Compagnie Générale du Basalte’ [1] by re-melting rocks (petrurgy). Today, several petrugical companies are active in Europe, producing building tiles, obtained by pressing or casting, pipes and bends by centrifuging, and glassy insulation fibers (rocks wool). Iron-rich glasses and glass-ceramics were developed

for the nuclear waste disposal [2–5] and more recently, for the vitrification of various hazardous industrial wastes [6–20].

The iron-rich compositions often show a tendency to spontaneous crystallization. This phenomenon increases the apparent viscosity of the melt [12,21,22] and might generate problems during the forming process [1]; also, the crystalline structure may become inhomogeneous and coarse. In order to overcome these phenomena, the sinter-crystallization technique was successfully applied [8,16,17,20].

The basaltic and basaltic related igneous rocks can be separated in two main groups: subalkaline and alkaline [23]; the first group is constituted by the tholeiitic and calcalkaline basalts, whereas the second – by the alkaline and alkaline-olivine basalts. Until now, the petrugy has mostly used tholeiitic basalts or diabasic rocks [24–28], which, due to their higher viscosity, are characterized by a reduced tendency to spontaneous crystallization. On the other hand, the low viscosity alkaline basalts appear more appropriated

* Corresponding author. Tel.: +359 2 979 2552; fax: +359 2 971 2688.
E-mail address: karama@ipc.bas.bg (A. Karamanov).

for the production of sintered ceramic and glass-ceramic materials.

The aim of present work is to obtain sintered glass-ceramics by using alkaline-olivine tuffs from Southern Anatolia. The kinetics of phase formation and the sintering behavior were studied in air and in nitrogen atmospheres by differential thermal analysis (DTA) and dilatometry, respectively. The crystalline phases formed were identified by X-ray diffraction.

2. Experimental

In a previous work [29], it was shown that, due to its initial porosity and elevated amount of amorphous phase (60–70 wt%) the basaltic tuff may be easily crushed and milled and that the crystal phases (mainly pyroxene, olivine and plagioclase) melt in the range of 1370–1480 K. These characteristics emphasize the possibility of applying simple and low-temperature melting procedure.

In the present study, the tuffs were crushed for few minutes in an agate mortar; then about 100 g of the obtained powder was melted in corundum crucible for 30 min at 1623 K and the melt was quenched in water. The resulting glass frit was milled below 75 μm .

The chemical composition was evaluated by XRF technique (Spectro XEPOS). The analysis show the following results (wt%): SiO_2 – 43.18 ± 0.08 , TiO_2 – 3.34 ± 0.01 , P_2O_5 – 0.96 ± 0.03 , Al_2O_3 – 13.15 ± 0.04 , Fe_2O_3 – 13.49 ± 0.04 , CaO – 9.67 ± 0.05 , MgO – 8.48 ± 0.07 , Na_2O – 4.27 ± 0.19 , K_2O – 2.78 ± 0.01 .

The crystallization kinetics was studied by DTA (Netzsch STA 409) technique at 5, 10, 15 and 20 K/min. The experiments were carried out in corundum crucibles using 80–110 mg single bulk samples from the parent frit and corundum powder as reference.

The activation energy of crystallization, E_C , was evaluated by the Kissinger equation [30]:

$$\ln \left(\frac{v}{T_p^2} \right) = \frac{-E_C}{RT_p} \quad (1)$$

where T_p is the crystallization exotherm peak temperature and v is the heating rate.

The Avrami parameter, m , was evaluated by the Ozawa equation [30]:

$$\frac{d[\ln(-\ln(1-\alpha))]}{d(\ln v)} \Big|_T = -m, \quad (2)$$

where the degree of transformation is estimated at a fixed temperature, T , from exotherms obtained at different v . α value is calculated as the ratio of partial area of the crystallization peak at T to its total area.

m was also estimated by the Augis–Bennet equation [30]:

$$m = \frac{(2.5/\Delta w)}{(RT_p^2/E_C)}, \quad (3)$$

where Δw is the width of the crystallization exotherm at half peak height.

The crystallization and sintering behaviors of the glass powder were investigated at 10 K/min heating rate in air and nitrogen atmosphere (1 L/min N_2 flow) by DTA and differential dilatometer (Netzsch 402 ED), respectively. A 100 mg powder samples were used in the DTA experiments, while the densification was studied by 10/4/4 mm^3 ‘green’ samples, pressed at 100 MPa.

The formed crystalline phases were determined by XRD technique (Philips-1830 apparatus and $\text{Cu K}\alpha$ radiation). The crystalline fraction was estimated by comparing the intensity of amorphous halo in the spectra of parent glass and glass-ceramics at 2θ values of 25 and 28 [31]. The method is based on the statement that the decreasing of scattering intensity of amorphous phase in the crystallized samples is proportional to the amount of formed crystal phase.

3. Results

Fig. 1 shows the DTA results of bulk sample in air and powder samples in air and nitrogen atmospheres, recorded at 10 K/min, while Fig. 2 presents the traces of bulk samples at different heating rates. Figs. 3 and 4 show the corresponding results for the activation energy of bulk crystallization, E_C , by Eq. (1) and the Avrami parameter, m , by Eq. (2), respectively. Table 1 summarized the m values, obtained by Eq. (3).

The dilatometric sintering curves in air and nitrogen atmospheres are depicted in Fig. 5.

The XRD spectra of the obtained sintered samples are plotted in Fig. 6 obtained: (a) in air atmosphere and (b) in nitrogen atmosphere.

4. Discussion

The DTA results of bulk and powder samples (Fig. 1) show an unusual crystallization behavior: the bulk sample has a higher crystallization trend than the powder samples, both in air and nitrogen atmospheres. The bulk sample shows glass-transition temperature, T_g , at about 910 K, sharp and intensive crystallization exo-effect with peak temperature, T_p , at 1095 K, liquids temperature, T_l , at 1397 K and two melting endo-effects at 1424 and 1468 K. The two powder samples show similar T_g and T_l , while T_p occur at higher temperatures.

The glass forming ability of the bulk sample was evaluated by the Hruby coefficient, $K_H = (T_p - T_g)/(T_l - T_p)$, and by the T_g/T_l ratio [32,33]. K_H has a low value of 0.63, which indicates a very high crystallization trend, whereas the T_g/T_l ratio of 0.65 is typical of a stable glass with a tendency to surface crystallization [34].

In order to clarify this apparent contradiction, the kinetics of phase formation in the bulk was studied at different heating rates. The obtained high value for E_C , 590 ± 20 kJ/mol, may be related to the elevated viscosities in the DTA crystallization temperatures interval. In fact,

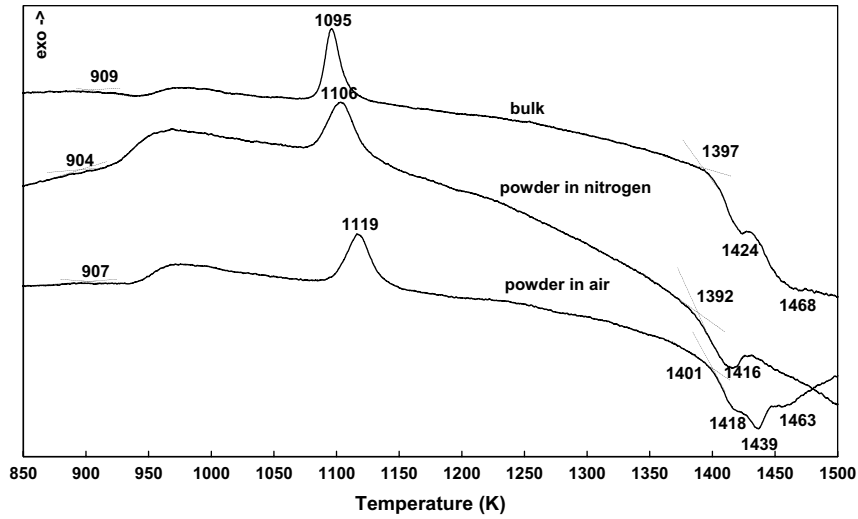


Fig. 1. DTA traces of bulk sample in air and powder samples in air and nitrogen atmospheres.

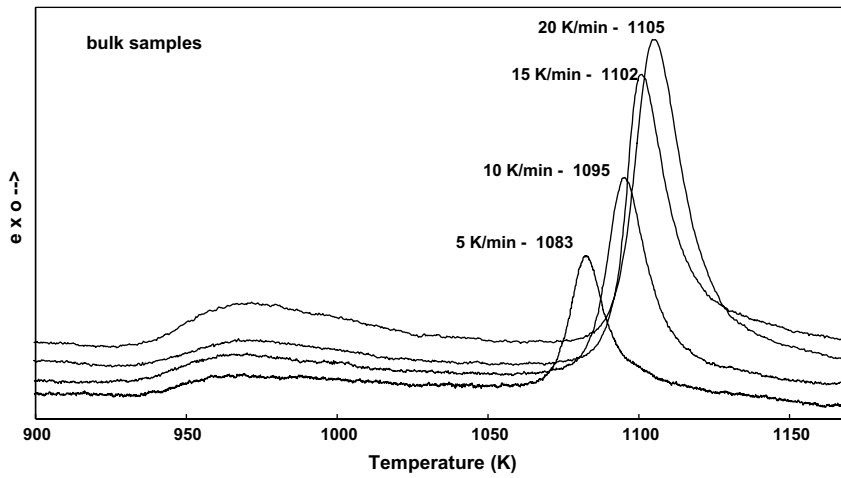


Fig. 2. DTA traces of bulk samples at different heating rates.

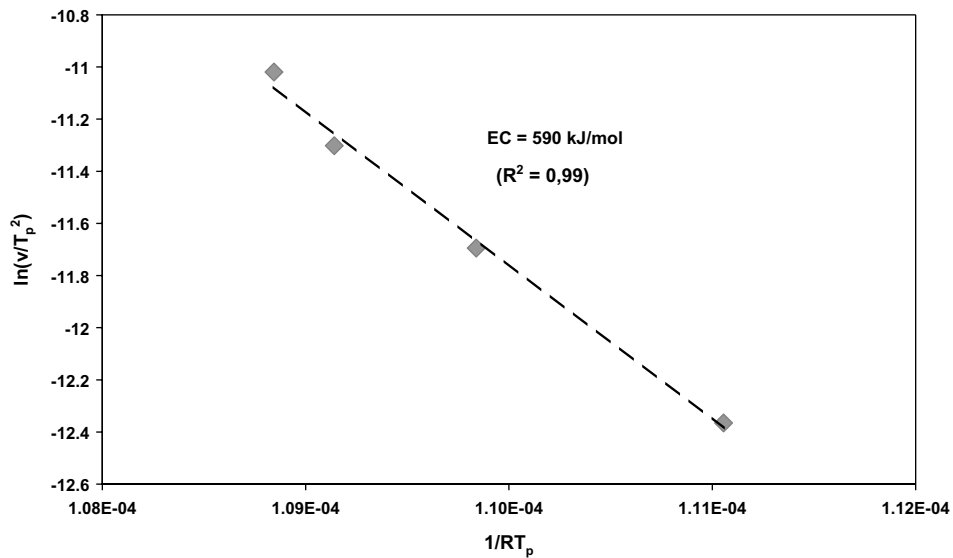


Fig. 3. Kissinger plot of the activation energy of crystallization.

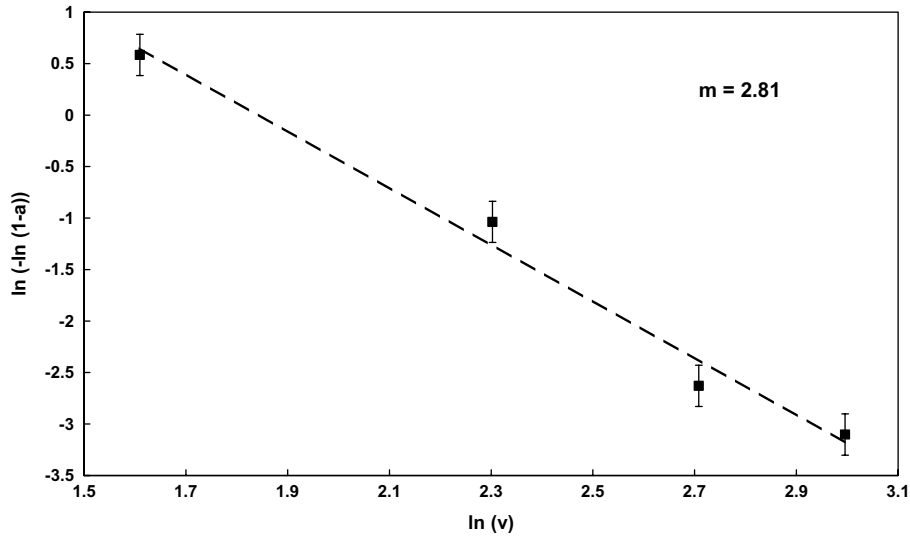


Fig. 4. Ozawa plot of the Avrami parameter.

Table 1
Values of the Avrami parameter by Augis–Bennet method

Heating rate (K/min)	5	10	15	20
Avrami parameter	3.1	2.9	2.8	2.7

in other iron-rich glass compositions, where K_H value is higher and the phase formation takes place at lower viscosity, E_C has lower value [9,11,15,16,25–27]. The reaction order, calculated by both Ozawa and Augis–Bennet methods, shows a value of ≈ 3 , corresponding to three-dimensional growth on fixed number of previously formed nuclei [30–32]. This crystallization behavior is typical for several iron-rich glasses [7,10,11,15] and may be explained by a liquid–liquid immiscibility of the melt at high temperature [35]. Then, during the cooling the iron-rich phase

promotes formation of a spinel crystal phase; the spinel crystals act as nuclei for the crystallization of the main crystal phases [11,35]. The number of formed spinel crystals depends on the melt composition and the quenching conditions.

The absence of a nucleation process near the glass-transition temperature was highlighted by additional DTA experiments, where bulk samples were held for 1 h at 910, 930 and 950 K, respectively, and then heat-treated at 10 K/min heating rate. No shift at lower temperatures of T_p was observed, showing that no additional nuclei formation occurred [30,31]. It was concluded that, due to spontaneous and rapid bulk crystallization, the investigated basalt tuff is not suitable for producing glass-ceramics by controlled bulk crystallization. For this reason, the sinter-crystallization technique was preferred.

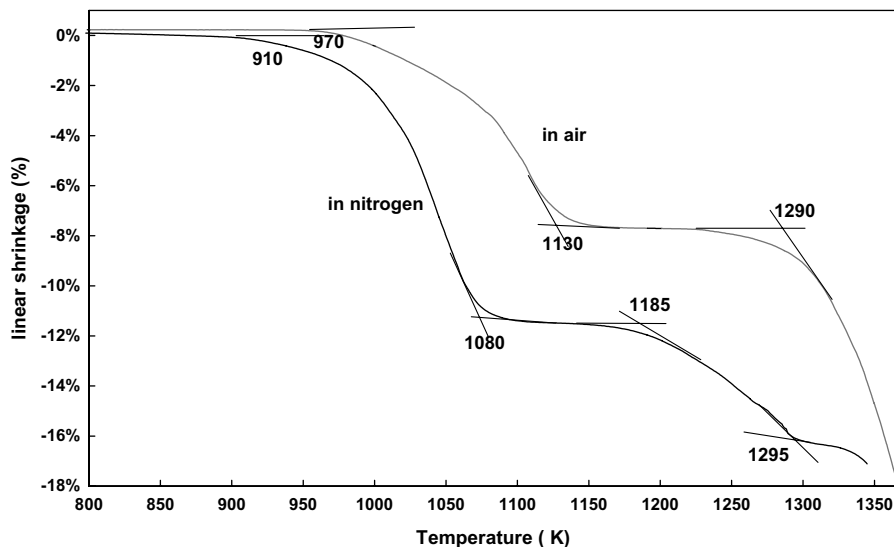


Fig. 5. Dilatometric sintering curves in air and nitrogen atmospheres.

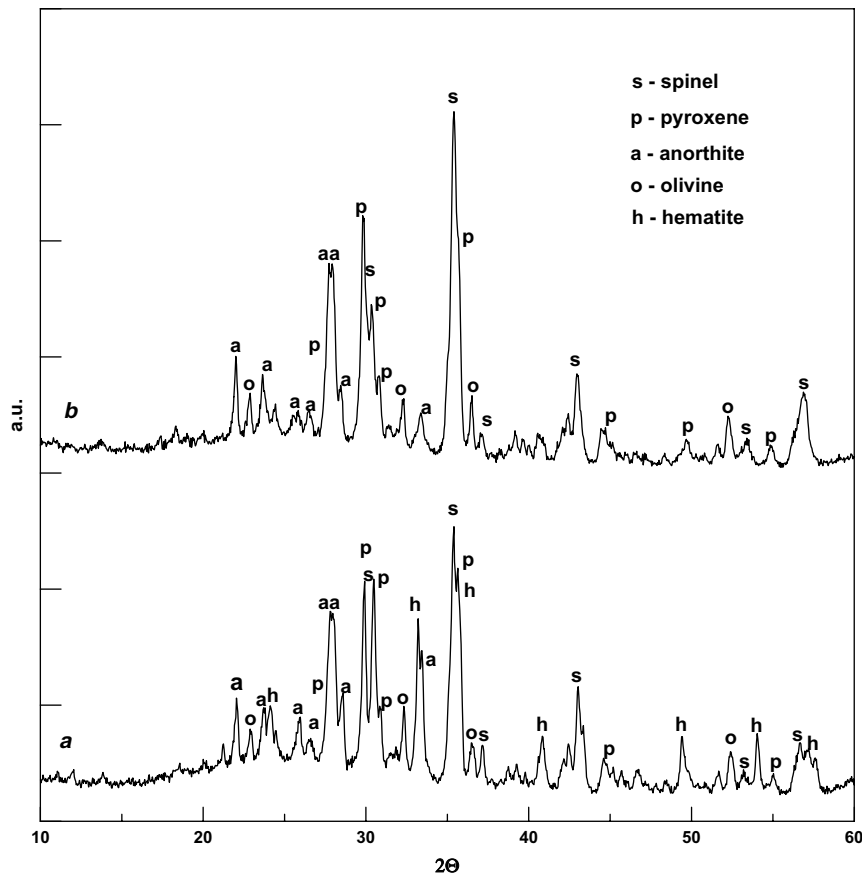


Fig. 6. XRD spectra of the sintered in air atmosphere and nitrogen atmosphere samples.

In previous works, it was demonstrated that the phase formation rate in iron-rich compositions depends on the $\text{Fe}^{2+}/\text{Fe}^{3+}$ ratio: the closer is this ratio to magnetite ($\text{FeO} \cdot \text{Fe}_2\text{O}_3$) value of 0.5 the higher is the crystallization trend [3,6,9,10,24,28]. The $\text{Fe}^{2+}/\text{Fe}^{3+}$ ratio also influences the sinter-crystallization of the glass powders [8,16,17,20]. In air atmosphere, the formation of magnetite spinels is inhibited by surface Fe^{2+} oxidation and the crystallization rate is reduced; at higher temperature the formation of hematite (Fe_2O_3) takes place. As a result, the DTA peaks of powder samples in air show a lower intensity and occur at 70–90 K higher temperatures than the bulk sample. On the other hand, the phase formation mechanism in powders, treated in nitrogen atmosphere, is similar to one in the bulk.

The sintering in air was obtained at higher temperature than in nitrogen [17]. This result also may be explained by the oxidation process, because the transformation of modifier FeO into intermediate Fe_2O_3 increases the viscosity and the sintering temperature.

In the present work, the DTA traces of the powder samples show similar crystallization peaks in air and nitrogen atmospheres with a T_p shift of only 15 K for the sample in air. This different behavior compared to the previously studied iron-rich glasses can be attributed to the high percentage of TiO_2 in the basaltic composition, acting as nucleating agent in the iron-rich glasses [6,24,31].

The dilatometric sintering curves show that in nitrogen atmosphere the sintering starts in the glass-transition temperature range and the linear shrinkage ($\Delta L/L_0$) is about 12% at 1080 K. After this temperature, the densification is inhibited by the crystal phase formation; further densification is achieved at 1185 K reaching $\Delta L/L_0$ of 16%. The deformation of the sample starts at 1330 K.

In air, the densification starts at 970 K and the sintering rate is significantly reduced by the oxidation of FeO and the linear shrinkage is as much as 7% at 1130 K. The sintering starts again at 1290 K and the end of the densification ($\sim 16\% \Delta L/L_0$) overlaps with the beginning of the deformation, at about 1360 K. Due to Fe^{2+} oxidation, the samples sintered in air have a reddish brown color, while these ones obtained in nitrogen atmosphere are black.

The degree of crystallinity of the samples, sintered in air is $45 \pm 5 \text{ wt}\%$, with main crystalline phases being spinel (JCPDS card 75-1207), pyroxene (JCPDS card 72-1279), hematite (JCPDS card 85-0987), anorthite plagioclase (JCPDS card 73-0265) and olivine (JCPDS card 83-0087). The samples, sintered in nitrogen correspond to a crystallinity of $60 \pm 5 \text{ wt}\%$, with the same crystalline phase without hematite. The formation of hematite and the decreasing of the spinel and pyroxene phases in air can be related to the Fe^{2+} oxidation.

5. Conclusion

The studied alkaline basaltic glass shows an unusual crystallization behavior with an extremely high rate of phase formation in the bulk. A three-dimensional growth on a fixed number of previously formed nuclei is proposed as crystallization mechanism. The high value of the activation energy of crystallization, 590 ± 20 kJ/mol, can be related to the high viscosity during the phase formation.

The sintering of powder samples is reduced by the intensive crystallization, both in air and nitrogen atmospheres. In nitrogen atmosphere, the densification starts at lower temperature and the total crystallinity increases from 45 ± 5 wt% to 60 ± 5 wt%. The densification starts again at 1150–1250 K and completes at 1300–1350 K.

References

- [1] B. Locsei, Molten Silicates and their Properties, Akademiai Kiado, Budapest, 1970.
- [2] D.F. Bickford, C.M. Jantzen, J. Non-Cryst. Solids 84 (1986) 299.
- [3] D. Schreiber, B.K. Kochanowski, C.W. Shreberg, in: G.B. Mellinger (Ed.), Ceramic Transactions, Environmental and Waste Management Issues in the ceramic Industry, vol. 39, The American Ceramic Society, 1994, p. 141.
- [4] I.W. Donald, B.L. Metcalfe, R.N.J. Taylor, J. Mater. Sci. 32 (1997) 5851.
- [5] P. Hrma, J.V. Crum, D.J. Bates, P.R. Brecht, L.R. Greenwood, H.D. Smith, J. Nucl. Mater. 345 (2005) 19.
- [6] M. Pelino, C. Cantalini, J. Ma Rincon, J. Mater. Sci. 32 (1997) 4655.
- [7] M. Romero, J. Ma Rincon, J. Eur. Ceram. Soc. 18 (1998) 153.
- [8] A. Karamanov, G. Taglieri, M. Pelino, J. Am. Ceram. Soc. 82 (1999) 3012.
- [9] A. Karamanov, P. Piscicella, M. Pelino, J. Eur. Ceram. Soc. 20 (2000) 2233.
- [10] A. Karamanov, P. Piscicella, C. Cantalini, M. Pelino, J. Am. Ceram. Soc. 83 (2000) 3153.
- [11] A. Karamanov, M. Pelino, J. Non-Cryst. Solids 281 (2001) 139.
- [12] A. Karamanov, R. Gioacchino, M. Pelino, Glass Technol. 43 (2002) 34.
- [13] M. Pelino, A. Karamanov, P. Piscicella, D. Zannetti, S. Crisucci, Waste Manage. 22 (2002) 945.
- [14] T.W. Cheng, Chemosphere 50 (2003) 47.
- [15] A.A. Francis, R.D. Rawlings, R. Sweeney, J. Non-Cryst. Solids 333 (2004) 187.
- [16] A. Karamanov, G. Taglieri, M. Pelino, J. Am. Ceram. Soc. 87 (2004) 1571.
- [17] A. Karamanov, G. Taglieri, M. Pelino, J. Am. Ceram. Soc. 87 (2004) 1354.
- [18] P.M. Suresen, M. Pind, Y.Z. Yue, R.D. Rawlings, A.R. Boccaccini, E.R. Nielsen, J. Non-Cryst. Solids 351 (2005) 1246.
- [19] Th. Kehagias, Ph. Komninou, P. Kavouras, K. Chrissafis, G. Nouet, Th. Karakostas, J. Eur. Ceram. Soc. 26 (2006) 1141.
- [20] A. Karamanov, M. Aloisi, M. Pelino, J. Hazard. Mater. 140 (2007) 333.
- [21] I. Vicente-Mingarro, J. Ma. Rincon, P. Bowles, R.D. Rawlings, P.S. Rogers, Glass Technol. 33 (1992) 49.
- [22] M.R. James, N. Bagdassarov, K. Muller, H. Pinkerton, J. Volcanol. Geotherm. Res. 132 (2004) 99.
- [23] S.A. Morse, Basalts and Phase Diagrams, Springer, New York/Heidelberg/Berlin, 1982.
- [24] H. Beall, H.L. Rittler, Ceram. Bull. 55 (1976) 579.
- [25] V. Znidarsic-Pongarac, D. Kolar, J. Mater. Sci. 26 (1991) 2490.
- [26] S. Yilmaz, O.T. Özkan, V. Günay, Ceram. Int. 22 (1996) 477.
- [27] G. Bayrak, S. Yilmaz, Ceram. Int. 32 (2006) 441.
- [28] D.J.M. Burkhard, T. Scherer, J. Non-Cryst. Solids 352 (2006) 3961.
- [29] S. Ergul, M. Akyildiz, A. Karamanov, Ind. Ceram (in press).
- [30] C.S. Ray, D.E. Day, in: Nucleation and Crystallization in Liquids and Glasses, Am. Ceram. Soc. 30 (1992) 207.
- [31] Z. Strnad, Glass-Ceramic Materials, Elsevier, Amsterdam, 1986.
- [32] I. Gutzow, J. Shmelzer, The Vitreous State – Structure, Thermodynamics, Rheology and Crystallisation, Springer, Berlin/New York, 1995.
- [33] I. Avramov, E.D. Zanotto, M.O. Prado, J. Non-Cryst. Solids 320 (2003) 9.
- [34] P.F. James, J. Non-Cryst. Solids 73 (1985) 517.
- [35] W. Höland, G. Beall, Glass-Ceramics Technology, The American Ceramics Society, Westerville, 2002.